

Control of spin in quantum dots with non-Fermi liquid correlations

Alessandro Braggio¹, Maura Sasseti¹ and Bernhard Kramer²

¹ Dipartimento di Fisica, INFN, Università di Genova, Via Dodecaneso 33, 16146 Genova, Italy

² I. Institut für Theoretische Physik, Universität Hamburg, Jungiusstraße 9, 20355 Hamburg, Germany

(July 18, 2001)

Spin effects in the transport properties of a quantum dot with spin-charge separation are investigated. It is found that the non-linear transport spectra are dominated by spin dynamics. Strong spin polarization effects are observed in a magnetic field. They can be controlled by varying gate and bias voltages. Complete polarization is stable against interactions. When polarization is not complete it is power-law enhanced by non-Fermi liquid effects.

PACS numbers: 73.63.Kv, 71.10.Pm, 72.25.-b

Spin phenomena in transport properties of low-dimensional quantum systems have become a subject of increasing interest [1,2]. Several fundamental effects have been predicted when controlling transport of electrons one by one in quantum dots as, for instance, spin blockade due to selection rules [3] and parity effects in the Coulomb blockade [4,5]. There are also perspectives of applications in spin-electronics, quantum computing and communication [6]. Previous works have been focusing on spin transport in two dimensional (2D) quantum dots connected to non-interacting leads and in the presence of a magnetic field [7], including also an oscillating magnetic electron spin resonance component [8]. Spin transport in circuits with ferromagnetic elements and in the presence of a Luttinger-liquid interaction [9–11] have been considered. Of fundamental interest is the spin control of electron transport in the presence of correlations since in nanoscale devices the latter are very important.

In the present paper, we derive a general theory for spin and charge transport through a quantum dot formed in a Luttinger liquid. We consider spin effects in the presence of a magnetic field. Specifically, we investigate to what extent non-Fermi liquid behaviour influences spin polarization. We find that spin-charge separation strongly affects the current-voltage characteristics. The spin leads to rich structure in the non-linear differential conductance that reflects both the collective spin density excitations and the orientations of the total spin in the quantum dot. A magnetic field in the quantum dot can spin-polarize the current strongly. This can be controlled by varying gate- or bias-voltages. Full spin polarization can be achieved. Non-complete polarization is power-law enhanced by the non-Fermi liquid correlations.

We start from a clean Luttinger liquid with spin. The charge interaction parameter is $g_\rho = (1+2V(0)/\pi v_F)^{-1/2}$ with v_F the Fermi velocity and $V(q)$ the Fourier transform of the electron interaction ($\hbar = 1$). For the exchange interaction, we assume $g_\sigma = 1$. The interacting 1D electrons are mapped, via bosonization, to a harmonic Hamiltonian [12]. The low-energy excita-

tions are charge and spin density waves, with dispersions $\omega_\nu(q) = v_F|q|/g_\nu \equiv v_\nu|q|$. Here, $\nu = \rho, \sigma$ label charge (ρ) and spin (σ). Spin-charge separation implies $v_\rho \neq v_\sigma$. The slowly varying (on the scale of $2\pi k_F^{-1}$) parts of the densities are given in terms of field operators $\Theta_\nu(x)$, $\nu(x) = \rho_\uparrow(x) + p_\nu \rho_\downarrow(x) \approx \nu_0 + \sqrt{2/\pi} \partial_x \Theta_\nu(x)$, with $p_\rho = +$, $p_\sigma = -$ and the mean charge and spin densities $\rho_0 = 2k_F/\pi$ and $\sigma_0 = 0$, respectively.

The quantum dot is formed by barriers $(U_t/\rho_0)\delta(x-x_i)$ at positions $x_1 < x_2$ given by the tunneling Hamiltonian

$$U_t \sum_{\alpha=0,1} \prod_{\nu} \cos \frac{\pi}{2} (N_\nu^- + \nu_0 d - \alpha) \cos \frac{\pi}{2} (N_\nu^+ - \alpha) \quad (1)$$

with $N_\nu^\pm = [\Theta_\nu(x_2) \pm \Theta_\nu(x_1)]\sqrt{2/\pi}$. Physically, N_ρ^- is the deviation of the number of electrons from the mean value, $n_0 = d\rho_0$, in the interval $d \equiv x_2 - x_1$. The excess charge then is $Q = -eN_\rho^-$, and the component of the total spin of the electrons parallel to the quantization axis (assumed parallel to the 1D system) $S = N_\sigma^-/2$. The numbers of imbalanced electrons and spins between the leads are N_ρ^+ and N_σ^+ , respectively. The coupling to the source-drain bias V and the gate voltage V_g is described by $H_V = -e(VN_\rho^+/2 + V_g N_\rho^- \delta)$, with δ the ratio between gate and total capacitances. The effect of an external magnetic field is described by a local Zeeman term in the region between the barriers, $H_B = -g_B \mu_B B N_\sigma^-/2 \equiv -E_B N_\sigma^-/2$, with the Landé-factor g_B [7,8].

The currents are calculated as the stationary limits of transferred charges and spins $I_\nu = I_\uparrow + p_\nu I_\downarrow = (e/2) \lim_{t \rightarrow \infty} \langle \dot{N}_\nu^+(t) \rangle$. The brackets include both thermal and statistical averages over the collective modes at $x \neq x_1, x_2$ with the density matrix reduced to N_ν^\pm [5].

For obtaining the non-linear current-voltage characteristics we consider the dynamics of the system described by the variables N_ν^\pm under the influence of the external fields in the 4D periodic potential Eq. (1). For high barriers, tunneling between nearest-neighbored minima dominate, with amplitude Δ that is related to U_t via the WKB-approximation [13]. These correspond to processes $N_\rho^- \rightarrow N_\rho^- \pm 1$ and $N_\sigma^- \rightarrow N_\sigma^- \pm 1$ associated

with changes of charge and spin numbers in the dot, respectively, and $N_\rho^+ \rightarrow N_\rho^+ \pm 1$ that transfer current. We consider sequential tunneling with the temperature much smaller than the dot level spacing. This can be described by a master equation for charges and spins with rates,

$$\Xi(E) = \sum_{n,m=-\infty}^{+\infty} W_n^\rho(\epsilon_\rho) W_m^\sigma(\epsilon_\sigma) \gamma^{(g)}(E - n\epsilon_\rho - m\epsilon_\sigma), \quad (2)$$

where the tunneling rate of a single barrier

$$\gamma^{(g)}(E) = \frac{\Delta^2}{4\omega_c} \left(\frac{\beta\omega_c}{2\pi} \right)^{1-1/g} \left| \Gamma \left(\frac{1}{2g} + \frac{i\beta E}{2\pi} \right) \right|^2 \times \frac{e^{-|E|/\omega_c} e^{\beta E/2}}{\Gamma(1/g)} \quad (3)$$

depends on the effective interaction parameter $g/2 = g_\rho g_\sigma / (g_\rho + g_\sigma)$ and the frequency cutoff ω_c . The weights, $W_n^\nu(\epsilon_\nu)$, at the discrete energies ϵ_ν are ($\beta^{-1} \equiv k_B T \ll \epsilon_\nu$)

$$W_n^\nu(\epsilon_\nu) \approx \left(\frac{\epsilon_\nu}{\omega_c} \right)^{1/2g_\nu} \frac{\Gamma(1/2g_\nu + n)}{n! \Gamma(1/2g_\nu)} e^{-\epsilon_\nu n / \omega_c} \theta(n). \quad (4)$$

In order to understand the rather complex behaviour of the transport spectra it is useful to recall the characteristic energy scales in (2). These are the *discretization energies* corresponding to charge and spin modes in the quantum dot relative to the energy of the ground state,

$$\epsilon_\nu \equiv \omega_\nu (q = \pi/d) = 2g_\nu E_\nu, \quad (5)$$

with the *addition energies* for charge and spin

$$E_\nu = \pi v_F / 2g_\nu^2 d. \quad (6)$$

Without interaction, the addition energies are $E_\rho = E_\sigma = \pi v_F / 2d = E_P \neq 0$, due to the Pauli principle, and the discreteness of the dot levels. On the other hand, for strong Coulomb interaction, $E_\rho \propto V (q \rightarrow 0) \gg E_\sigma$ [5].

The addition energies determine the ground state energy of n charges with the half-integer total spin $S \equiv s_n/2$, $E_0(n) = [E_\rho (n - n_g)^2 + E_\sigma s_n^2 - E_B s_n] / 2$. The reference particle number $n_g \equiv eV_g \delta / E_\rho + n_0$ is defined by the gate voltage. The energy differences of the many-body states of $n+1$ and n electrons are

$$\begin{aligned} \mu(n, s, l, m) &= \frac{E_\rho}{2} (2n + 1 - 2n_g) + \frac{E_\sigma}{2} (s_{n+1}^2 - s_n^2) \\ &\quad - \frac{E_B}{2} (s_{n+1} - s_n) + l\epsilon_\rho + m\epsilon_\sigma. \end{aligned} \quad (7)$$

Positive or negative integers l and m denote the differences of the numbers of charge and spin excitation quanta with the energies (5), respectively. These do not change neither the number of particles nor the total spin in the quantum dot. The energy differences $\mu(n, s, l, m)$ play the role of chemical potentials of the dot and define the transport regions. For symmetric bias, for instance, the

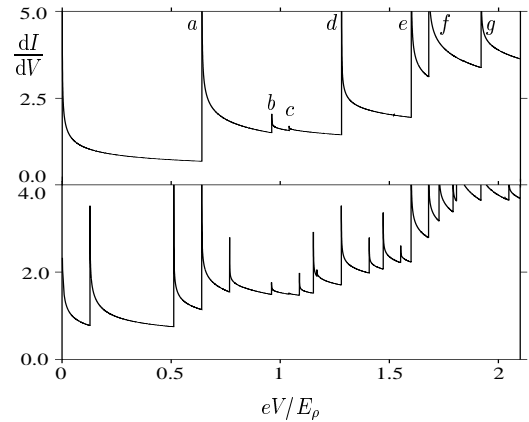


FIG. 1. Differential conductance dI/dV as a function of the source-drain bias eV/E_ρ for $g_\rho = 0.4$ ($\omega_c = 10^5 E_\sigma$, units $10^{-3} (\omega_c/E_\sigma)^{(g-1)/2g} e^2 \Delta^2 / 4\omega_c^2$). Top: $E_B = 0$, $n_g = 0.58$; bottom: $E_B = 0.4 E_\sigma$, $n_g = 0.548$.

condition $V/2 > \mu(n, s, l, m) > -V/2$ defines the allowed transport channels. For $V \rightarrow 0$ and $E_B \ll E_\sigma$ one finds the Coulomb blockade peaks at gate voltages V_g that correspond to $\mu(n, s, l, m)$. However, due to the spin, the separation of the peaks depend on the parity of n , $\Delta V_g^{n+1, n} = [E_\rho + (-1)^{n+1} (E_\sigma - E_B)] / e\delta$. Without interaction, one has to replace here $E_\rho = E_\sigma \equiv E_P$, in order to get the separation of the linear conductance peaks.

In the following, we consider the limit $T = 0$. Results for the differential conductances dI/dV for $E_B = 0$ and $E_B = 0.4 E_\sigma$ as functions of V are shown in Fig. 1. Zero bias voltage has been assumed at the position of a conductance peak corresponding to an n (even)-to- $(n+1)$ ground-state-to-ground-state transition. The differential conductance shows sharp peaks at bias voltages V_{nlsm} at which a new transport channel enters the above bias voltage window. Above V_{nlsm} , the conductance as a function of V drops according to the interaction-induced non-Fermi liquid power law $(V - V_{nlsm})^{1/g-2}$.

From (7) one can easily identify the spectral origins of the peaks in the conductance spectra. At low voltages, the spectra are completely dominated by spin excitations due to spin-charge separation. The discretization and addition energies corresponding to the spin are factors g_ρ and g_ρ^2 , respectively, smaller than those corresponding to the charge. For $B = 0$ peak (e) corresponds to a charge density excitation at ϵ_ρ , while (f) is due to the ground-state to ground-state transition at $E_\rho - E_\sigma$. All of the other peaks in Fig. 1 are spin-related. Because $g_\sigma = 1$ the transition at $2E_\sigma$ is degenerate with the spin density excitation at ϵ_σ (peak (a), with multiples (d) and (g)). A finite exchange would remove this degeneracy and discriminate between spin addition energies and spin density waves. The two small features (b) and (c) are combinations of the excitations (e) and (f) with E_σ , they corresponds to $\epsilon_\rho - 2E_\sigma$ and $E_\rho - 3E_\sigma$, respectively. In the non-interacting limit, the peaks in the

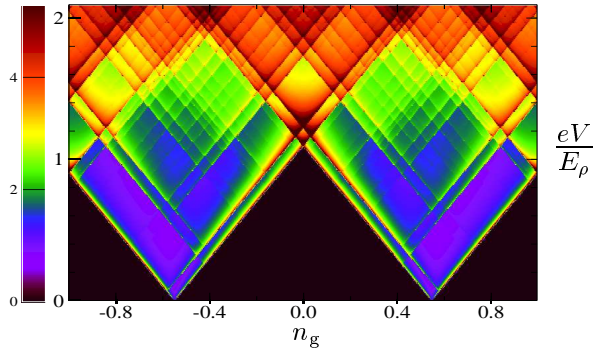


FIG. 2. Density plot of the differential conductance in the $(eV/E_\rho, n_g)$ -plane for interaction $g_\rho = 0.4$ and magnetic field $E_B = 0.4 E_\sigma$ ($\omega_c = 10^5 E_\sigma$, color code (left) with units $10^{-3}(\omega_c/E_\sigma)^{(g-1)/2g} e^2 \Delta^2 / 4\omega_c^2$).

non-linear differential conductance appear at bias voltages that are multiples of $4E_P$ due to the absence of spin charge separation. Apart from the peak at $V = 0$, all of the peaks are absent without electron interaction, for the bias voltages in Fig. 1 (top).

The spin-related features are even more strikingly displayed in the spectra for $E_B = 0.4 E_\sigma$ (Fig. 1 bottom). All of the peaks in Fig. 1 (top) acquire Zeeman side bands corresponding to energies $E_{\text{peak}} \pm E_B$. Exceptions are (b) and (c). They only have sidebands $E_{\text{peak}} + E_B$ since the initial states corresponding to the lower sidebands cannot be occupied by electrons entering the dot at $T = 0$.

As an example of the rich spin-related structure in the transport spectrum a density plot of the differential conductance in the $(eV/E_\rho, n_g)$ -plane for $E_B = 0.4 E_\sigma$ is shown in Fig. 2. The black regions correspond to the Coulomb blockade. When increasing the bias voltage the the excitation spectrum displays a considerable number of spin-related transitions. With non-vanishing exchange interaction, $g_\sigma \neq 1$, accidental degeneracies due to spin addition and excitation are lifted and the spectrum becomes even more complex.

Figure 3 shows the behaviour of a current peak for fixed bias, $I(n_g)$, when changing the magnetic field. As B is changed, peak height and position vary with periods $2E_\sigma$ and $4E_\sigma$, respectively (Fig. 3 bottom). This can be understood by considering the processes that contribute towards the current. We start by discussing the peak position for $V \rightarrow 0$. For small B and keeping n_g as to match the maximum of the peak (Fig. 3 top) one finds from (7) that with increasing B one has to adjust n_g to lower values $\propto -E_B/2$ since $s_{n+1} - s_n = +1$ which corresponds to the $s_n = 0 \rightarrow s_{n+1} = 1$ transition. When $E_B \geq 2E_\sigma$, the energy of the state $s_n = 2$ becomes lower than that of the $s_n = 0$ state such that transport gets now support from transitions $s_n = 2 \rightarrow s_{n+1} = 1$ with $s_{n+1} - s_n = -1$ while $s_{n+1} + s_n = 3$ instead of 1. When increasing B further, n_g has now to be adjusted to higher values $\propto +E_B/2$ in order to compensate for the Zeeman

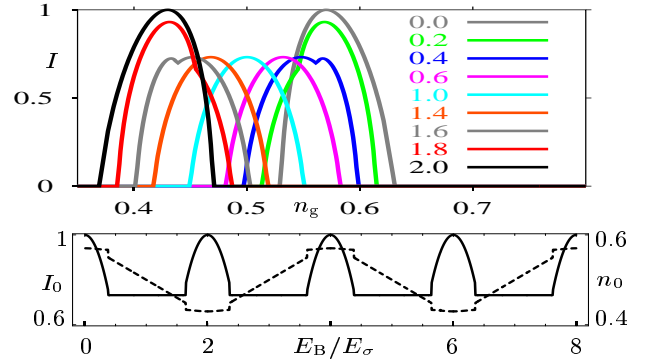


FIG. 3. Top: Current I , normalized to the value at $B = 0$, as a function of the gate voltage n_g for different magnetic fields E_B/E_σ (inset) for $g_\rho = 0.4$ and at $eV = 0.1 E_\rho$ ($\omega_c = 10^5 E_\sigma$). Bottom: position of maximum of peak, n_0 (dashed, right scale) and current at peak maximum, I_0 (full line, left scale) as a function of E_B/E_σ .

shift. The original position is reached after a total change of B corresponding to $E_B = 4E_\sigma$. For $V \neq 0$, the peak position remains unchanged as long as energies of the transitions are inside the interval $(-V/2, V/2)$.

For understanding the peak height we consider $V \neq 0$. The bias V gives the width of the current peak. First, we remember that for $E_B \ll eV$, the current is due to two transitions, namely $s_n = 0 \rightarrow s_{n+1} = \pm 1$. This leads to the asymmetry of the (non-spin polarized) peak for $E_B = 0$ that can be observed in Fig. 3 (top). When $E_B \approx eV$ the contribution of the ground-to-excited-state transition $s_n = 0 \rightarrow s_{n+1} = -1$ is suppressed. Further increasing B , the current peak becomes symmetric, completely polarized (cf. Fig. 4), its height is reduced and remains constant. For $E_\sigma \ll E_B < 2E_\sigma$ transport gets support also from transition $s_n = 2 \rightarrow s_{n+1} = 1$ such that the peak height starts to become again asymmetric and to increase until, exactly at $E_B = 2E_\sigma$, both contributions are equally important. Then, the current peak acquires the same shape as for $E_B = 0$, but reflected at $n_g = 1/2$. Increasing B produces oscillatory behavior due to further changes of the values of s_n and s_{n+1} . The current has its maximum value at $n_g = 1/2$ whenever E_B is an odd multiple of E_σ . This fully polarized current states are also reflected in the digital behaviour [15] displayed in Fig. 3 (bottom). The latter becomes less stable when increasing the bias voltage V .

Figure 4 shows the behaviour of the current polarization, $P = I_\sigma/I_\rho$. The top-left panel shows P as a function of the source-drain voltage for a given magnetic field and different interaction strengths, with n_g at the maximum of the linear conductance. The polarization is complete for $eV \leq 2E_B$, independently of the interaction. When $eV > 2E_B$, P decreases as a function of V according to a non-Fermi liquid power law and is higher for stronger interaction. Thus, correlations *enhance* the polarization when the latter is not complete.

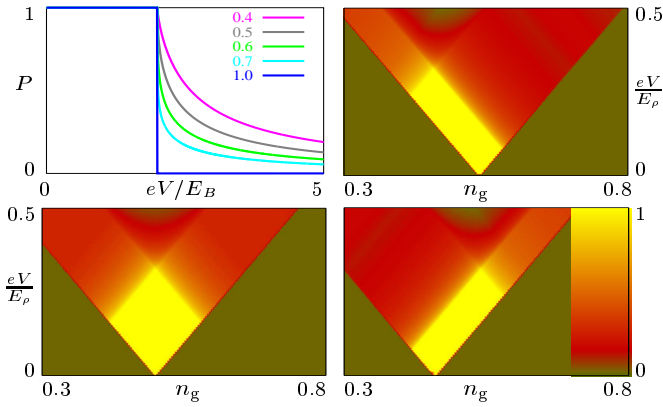


FIG. 4. Current polarization $P = I_\sigma/I_\rho$ for different interactions g_ρ (inset) as a function of eV/E_B for $E_B = 0.4 E_\sigma$ and n_g at the maximum of the conductance peak (top left); P in the plane $(eV/E_\rho, n_g)$ for $g_\rho = 0.4$ and magnetic field $E_B = 0.5 E_\sigma$ (top right), $E_B = E_\sigma$ (bottom left) and $E_B = 1.5 E_\sigma$ (bottom right, includes color code).

The other three panels of Fig. 4 show density-plots of the polarization for fixed interaction. Details of the behaviour can be understood from the discussion related to Fig. 3. Varying the magnetic field, complete polarization, $P = 1$ (yellow), is transferred between different regions of the (eV, n_g) -plane. The top-right panel corresponds to $E_B = 0.5 E_\sigma$ where the dominating $s_n = 0 \rightarrow s_{n+1} = 1$ channel leads to complete spin polarization near the left-hand edge of the region of non-zero current. Near $E_B = E_\sigma$ (bottom-left) the current peak is symmetrically spin polarized (for small V , yellow diamond). Increasing the magnetic field fully polarizes the right-hand edge of the current region ($E_B = 1.5 E_\sigma$, bottom-right). Exactly at $E_B = 2E_\sigma$ the two involved transport channels have equal weight and spin polarization is exactly zero, as for $E_B = 0$. By further increasing B , the behaviour of the polarization is reversed, $P = -1$. It can be displayed by the same panels, but in opposite direction. The periodicity of P with respect to E_B corresponds to $4E_\sigma$.

In conclusion, we have shown how one can control the spin properties of the transport through a 1D quantum dot embedded in a non-Fermi liquid by changing magnetic field, and gate- and source-drain voltages. This is due to the interaction that separates the energy scales of the charge and the spin excitations such that $E_\sigma \ll E_\rho$. Complete spin polarization can be achieved in spite of the presence of correlations. Once it is achieved, it is not influenced by the interaction. When polarization is not complete, it is enhanced by the non-Fermi liquid correlations. This shows that the electron spin is crucial for understanding non-linear transport in 1D quantum dots.

The above results have been obtained for $T = 0$. When $T > 0$, we expect temperature-induced Luttinger liquid power-law broadening of the conductance peaks, and correspondingly a smearing of the spin polarization features which is the subject of future work. At very low tempera-

tures, one would expect that coherent tunneling processes dominate. Including spin, these lead to the well-known quantum-dot Kondo physics which is not considered in our approach [14]. Therefore, the above results apply to temperatures higher than the Kondo temperature.

Our results for the transport spectra are consistent with several of the non-linear features observed recently in a one dimensional (1D) quantum dot formed by two impurities in a cleaved-edge overgrowth quantum wire [16]. More detailed experiments, however, are needed in order to test the above predictions, especially concerning the control of the spin. We expect that the effects can be observed in the transport through double barriers formed in cleaved-edge-overgrowth quantum wires, and in carbon nanotubes [17].

Acknowledgements: This work has been supported by Italian MURST via PRIN 2000, by the EU within TMR and RTN programmes, and by the DFG.

-
- [1] G.A. Prinz, *Physics Today* **282**, 58 (1995); *Science* **282**, 1660 (1998).
 - [2] J.M. Kikkawa, and D.D. Awschalom, *Phys. Rev. Lett.* **80**, 4313 (1998); D.D. Awschalom, and J.M. Kikkawa, *Phys. Today* **52**, 33 (1999).
 - [3] D. Weinmann, W. Häusler, and B. Kramer, *Phys. Rev. Lett.* **74**, 984 (1995);
 - [4] S. Tarucha, D.G. Austing, T. Honda, R.J. van der Hage, and L.P. Kouwenhoven, *Phys. Rev. Lett.* **77**, 3613 (1996).
 - [5] T. Kleimann, M. Sassetti, B. Kramer, and A. Yacoby, *Phys. Rev. B* **62**, 8144 (2000).
 - [6] A. Imamoglu, D.D. Awschalom, G. Burkard, D.P. DiVincenzo, D. Loss, M. Sherwin, and A. Small, *Phys. Rev. Lett.* **83**, 4204 (1999).
 - [7] P. Recher, E.V. Sukhorukov, and D. Loss, *Phys. Rev. Lett.* **85**, 1962 (2000).
 - [8] H.A. Engel, and D. Loss, *Phys. Rev. Lett.* **86**, 4648 (2001).
 - [9] A. Brathaas, Y. Nazarov, and G.E.W. Bauer, *Phys. Rev. Lett.* **84**, 2481 (2000).
 - [10] Q. Si, *Phys. Rev. Lett.* **81**, 3191 (1998).
 - [11] L. Balents, and R. Egger, *Phys. Rev. Lett.* **85**, 3464 (2000).
 - [12] J. Voit, *Rep. Progr. Phys.* **58**, 977 (1995).
 - [13] A. Braggio, M. Grifoni, M. Sassetti, and F. Napoli, *Europhys. Lett.* **50**, 236 (2000).
 - [14] A. Furusaki, *Phys. Rev. B* **57**, 7141 (1998).
 - [15] M. Ciorga, A.S. Sachrajda, P. Hawrylak, C. Gould, P. Zawadzki, S. Jullian, Y. Feng, and Z. Wasilewski, *Phys. Rev. B* **61**, R16315 (2000).
 - [16] O.M. Auslaender, A. Yacoby, R. de Picciotto, K.W. Baldwin, L.N. Pfeiffer, and K.W. West, *Phys. Rev. Lett.* **84**, 1764 (2000).
 - [17] H.W.Ch. Postma, M. de Jonge, Z. Yao, and C. Dekker, *Phys. Rev. B* **62**, R10653 (2000).